

Review Blood Flow Effects in Magnetic Resonance Imaging

Leon Axel¹

Although magnetic resonance (MR) has long been talked about as a noninvasive and apparently simple way to measure blood flow, practical realization of MR blood-flow measurement has not been fully accomplished. The principal reason for this is that blood flow affects the intensity of MR images in many nonlinear ways that depend both on details of the particular imaging technique and on blood vessel and flow geometry. Thus, the intensity of flowing blood may be increased or decreased relative to stationary blood, depending on the particular imaging technique used and the flow velocity. Only recently have efforts been made to design imaging pulse sequences that would have clearly identifiable flow effects that could be used to determine blood flow. Such pulse sequences have limitations and have only been quantitatively tested *in vitro* on artificial flow systems.

In this review, the principal flow effects in current MR imaging (MRI) techniques are presented. The first section is a general review of basic aspects of blood flow relevant to MRI and a brief summary of prior approaches to MR flow measurement and reported MRI flow effects. The second section contains a more detailed discussion of three basic underlying effects of flow that affect MRI: washout of saturated spins, displacement of excited spins, and phase shifts of excited spins due to motion along magnetic field gradients. The third section presents some experimental results to demonstrate the difference in washout effects observed with selective and nonselective refocusing pulses in spin-echo MRI. The final section considers some of the possible approaches to measurement of flow with MRI.

Blood Flow and Observed MR Flow Effects

Blood flow in the larger vessels (arteries and veins) must be considered separately from the microcirculation that provides tissue perfusion through capillaries. MRI shows clear effects from flow in large vessels, suggesting that it should allow measurement of blood flow; no convincing effects of tissue blood flow in MRI have yet been demonstrated. Thus MRI measurement of flow in major blood vessels is both an interesting and promising area for research. Although tissue perfusion is physiologically important, it is difficult to measure and direct MR studies of tissue perfusion are less promising at the moment. We will concentrate here on the MR effects of flow in major blood vessels.

Flow in the major blood vessels is neither constant in time nor constant across the lumen of the vessel [1]. The flow in the arteries is pulsatile, with most of the flow occurring during systole. Thus, the mean flow velocity is lower than the peak velocity (e.g., 20 cm/sec mean velocity vs. 120 cm/sec peak velocity in the dog aorta). Flow velocities decrease in the branch arteries, with mean flow velocities on the order of 10 cm/sec. Capillary blood flow is much steadier, with mean velocities on the order of 1 mm/sec or less. The microcirculation forms an interconnected network in tissue, with the blood volume typically a few percent or so of the tissue volume [2]; the mean transit time of the blood through the tissue (typically

Received June 18, 1984; accepted after revision August 29, 1984.

Dr. Axel is an Established Investigator of the American Heart Association and is supported in part by funds from the Southeast Pennsylvania Chapter.

¹ Department of Radiology, Hospital of the University of Pennsylvania, 3400 Spruce St., Philadelphia, PA 19104.

AJR 143:1157-1166, December 1984
0361-803X/84/1436-1157
© American Roentgen Ray Society

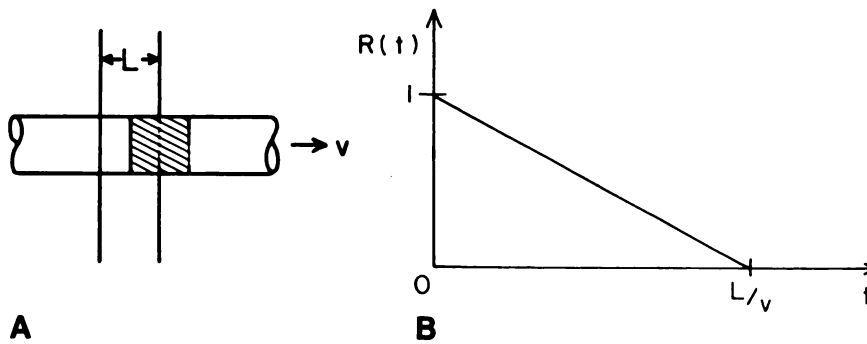


Fig. 1.—Plug flow (single velocity). Washout from rectangular profile imaging region (slice). A, Schematic representation of previously tagged (e.g., saturated or excited) fluid (shaded region) being washed out of slice of thickness, L , by flow of velocity, v . B, Fraction of spins remaining in slice, $R(t)$, after tagging at time $t = 0$.

a few seconds) is often a more useful concept than the velocity [3]. Flow in the veins is again somewhat unsteady, due to a combination of transmitted pulsations from the right heart, effects of respiratory maneuvers, and action of nearby muscles; mean velocities in the veins are somewhat lower than in the arteries. The profile of velocities in the lumen does not necessarily follow a Poiseuille flow parabolic profile. Although there is a boundary layer of relatively stagnant fluid near the wall, and the center of the vessel tends to have the most rapid flow, curvature and branching of vessels may produce asymmetry of axial velocity profiles and secondary flows. Even in the absence of these effects, the velocity profile is often flatter than a parabola. Blood flow is normally smooth [1]. However, in the presence of stenosis, such as due to atherosclerosis or valve disease, significant turbulence may appear downstream.

Although the major arteries and veins tend to run parallel to the long axis of the body and limbs, the course of branch vessels is more variable. Thus a vessel may intersect a transverse (or other) imaging plane at an oblique angle.

It was known long before the development of MRI that the signal produced by MR is affected by motion. Suryan [4] reported that for fluid flowing through a coil, the signal first increased and then decreased with increasing velocity, due to replacement of partly saturated (due to prior excitation) spins in the coil by fluid from upstream that had not been previously excited. With slow flow, the new spins were strongly magnetized and gave a strong signal, whereas with rapid flow, the upstream fluid was less completely magnetized due to less time spent in the magnet and gave a weaker signal. Hahn [5] found that motion resulted in decreased amplitude of spin-echo (SE) formation, due to inhomogeneity of the magnetic field. Carr and Purcell [6] further studied the dependence of SE amplitude on motion along a magnetic field gradient, due to acquired phase shifts; they showed that in echo trains, this only affects odd-numbered echoes. These two basic flow effects, namely washout of saturated spins and production of phase shifts by motion along a gradient, have been used to study flow in a variety of nonimaging MR techniques and have been applied to biologic systems, particularly by groups associated with Singer [7-11] and Battocletti [12-14]. Jones and Child [15] and Singer [16] have reviewed many of these approaches; a few specific papers will be mentioned here. Hahn [17] proposed using a switched-pulsed-gradient magnetic field to produce a phase shift of the SE, which would be proportional to the velocity along the

direction of the gradient. Stejskal [18] described the effect of pulsed magnetic field gradients on the phase of moving spins. Arnold and Burkhart [19] pointed out that motion of excited nuclei out of the region of the refocusing pulse will result in decreased SE amplitude. Packer [20] proposed a modification of the Carr-Purcell pulse sequence [6] that minimizes the effect on SE amplitude of diffusion relative to flow. Hayward et al. [21] used such a sequence to study flow velocity distributions, with pulsed magnetic field gradients. Garroway [22] demonstrated techniques to find velocity distributions using both washout of saturated spins and phase shifts of SEs due to motion along magnetic field gradients. He also proposed using selective excitation (by tailoring the range of exciting frequencies in the presence of a magnetic field gradient) in flow studies.

The development of MRI led to the observation of flow effects in the images of blood vessels [23]. The nature of the observed flow effects depends on the type of imaging technique used and the magnitude of the flow, as will be discussed further in the next section. Imaging techniques using detection of the signal as a free induction decay (FID) show effects from washout of saturated spins. When the time between excitations is on the order of or shorter than the tissue T_1 values, the effect of blood flow replacement of partially saturated spins in the slice being excited by fully magnetized spins from outside the slice will result in a stronger signal from the moving blood in vessels than from stationary blood, or even the surrounding tissues [24]; this is exactly analogous to the nonimaging results of Suryan [4]. With imaging using the signal detected as a spin echo, additional effects of flow also become important. At low velocities, a similar effect of increased signal due to washout of partially saturated spins can be observed [25]. At higher velocities, the signal intensity decreases with increasing velocity; that this is due in part to dephasing effects of motion along the imaging and other magnetic field gradients is seen by the fact that the second spin echo of a pair has greater amplitude than the first [26], as expected from the work of Carr and Purcell [6]. Part of the loss of signal is also due to washout of the excited spins from the refocusing region [19] when selective refocusing pulses [27] are used. Phase shifts with resulting changes in signal strength can also be produced by secondary flow within the imaging plane [28]. A different flow effect may be seen with SE imaging using nonselective 180° refocusing pulses, as they act like inverting pulses outside the region being imaged. This may result in partial saturation of blood

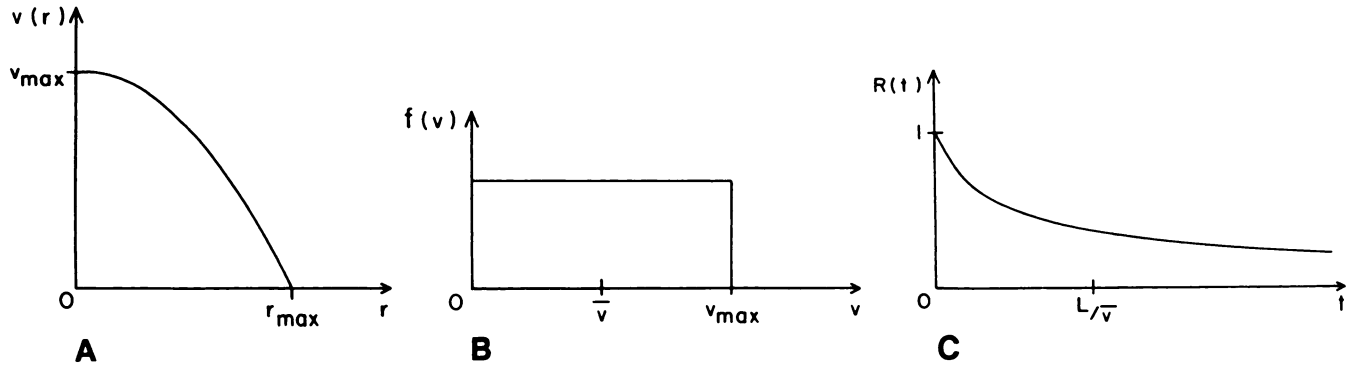


Fig. 2.—Poiseuille (simple laminar) flow washout from rectangular slice. A, Parabolic profile of velocity, v , as function of radial position, r , in vessel; r_{\max} is radius of vessel. B, Corresponding distribution function of velocities $f(v)$. C,

Fraction of spins remaining in slice, $R(t)$, after tagging at time $t = 0$ for this velocity distribution and geometry as in fig. 1.

flowing into the region to be imaged, with a corresponding decrease in the signal strength [29].

Although the flow effects in MRI are useful for delineation of normal and abnormal vascular anatomy and qualitative assessment of flow [30, 31], few attempts have been made to design MRI sequences specifically to evaluate blood flow. Singer and Crooks [32] have used a pulse sequence with a selective saturation pulse preceding a conventional imaging excitation pulse; varying the delay between these pulses allows variable amounts of washout and thus gives a measure of flow velocity. It has been proposed that the difference in signals after selective and nonselective preceding pulses can yield flow information [33]. Wehri et al. [29] subtracted images made with selective and nonselective preceding saturation pulses in order to cancel out the effects of stationary spins; the signal from the moving spins is again proportional to the degree of washout in the interval between the saturation and excitation pulses. Moran [34] has proposed using the phase shifts introduced in spin echoes from moving nuclei by balanced-gradient magnetic field pulses to produce a velocity-dependent image. Several groups [35–38] have implemented related velocity-dependent phase-sensitive images. Feinberg et al. [38] have proposed following moving excited spins by displacing a selective refocusing pulse to move with them; this discriminates against stationary spins and gives a measure of flow velocity, especially in conjunction with measurement of velocity-dependent phase shifts. This technique used synchronization with the cardiac cycle; George et al. [39] have examined some of the effects of pulsatile flow on MR signal strength.

Origins of Flow Effects in MRI

Washout of partially saturated or excited nuclei (spins) from the region being imaged (slice) is an important basic flow effect. Selective MR excitation in a limited region of space (used to define a slice) can be produced with a combination of an excitation pulse containing a narrow range of frequencies and a magnetic field gradient during excitation [22]. The result is "tagging" of the spins in the excited region both by their excitation (transverse magnetization), which will last for times on the order of the T2 relaxation time, and by their

partial saturation (loss of longitudinal magnetization), which will last for times on the order of the T1 relaxation time. Motion of these tagged spins can alter the resulting subsequent MR signal strength. The replacement of saturated spins within the slice by spins from outside the slice in times less than or on the order of T1 will result in a change in the signal produced by a subsequent excitation pulse. If the spins being washed in from outside the slice are less saturated than the spins being washed out, the signal will increase, other factors being equal, as has long been known from nonimaging MR studies [4]. Although this increase in signal has sometimes been called "paradoxical enhancement," there is nothing paradoxical about it. Consider the mechanical washout of fluid from the slice being imaged. For a single velocity, v , at right angles to the plane of the slice and a square slice profile with thickness L , the fraction of spins remaining in the slice after a time t , $R(t)$, is given by (fig. 1):

$$R(t) = \begin{cases} 1 - t \cdot (v/L), & t \leq L/v \\ 0, & t > L/v \end{cases} \quad (1)$$

Thus, the fraction of spins remaining in the slice decreases linearly until all the spins have been washed out, at a time L/v . For a range of velocities, as in Poiseuille flow, the decrease will be nonlinear (fig. 2). For a vessel at another angle to the slice, only the component of the velocity perpendicular to the slice will appear in this equation. For pulsatile flow, the amount of washout will depend on the mean velocity during the time t .

For this simple geometry, the signal resulting from a selective saturation pulse followed after a time, TD, by a selective excitation pulse will be given by the combination of the signal from the partially saturated spins remaining in the slice, weighted by $R(TD)$, and the signal from the unsaturated spins being washed in from upstream, weighted by $1 - R(TD)$. The amount of signal from the "saturated" spins will depend on the amount of recovery of longitudinal magnetization, given by a factor of $1 - \exp(-TD/T1)$ (fig. 3). The selective saturation pulse could be either a special pulse used to produce saturation [31, 33] or just the preceding pulse in an ordinary saturation-recovery pulse sequence. Note that for increasing delay times, TD, and a fixed velocity, the signal increases from zero until its maximum at the washout time. However,

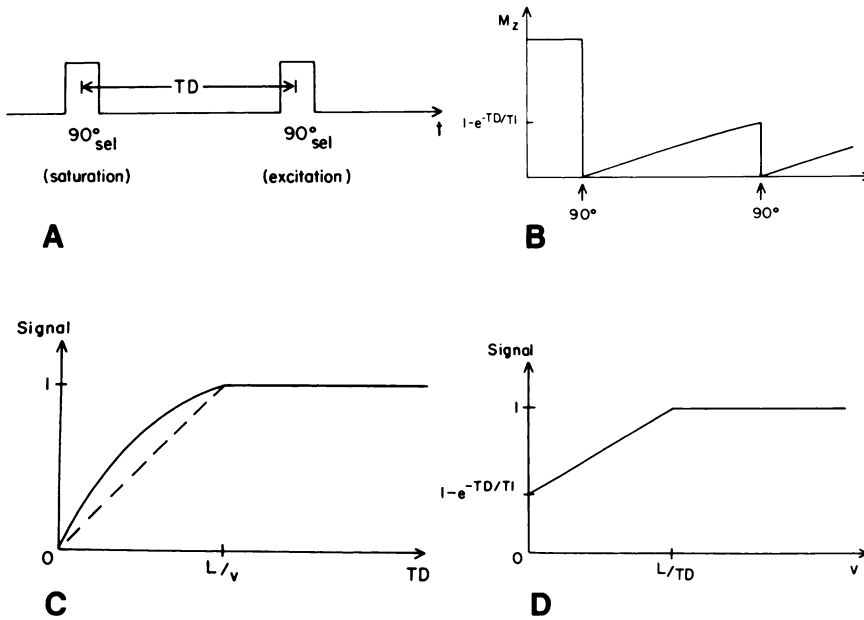


Fig. 3.—Effect of washout as in fig. 1, with tagging by saturation. A, Schematic RF pulse sequence: selective saturation pulse followed after delay of TD by selective excitation pulse at same location. B, Longitudinal magnetization, M_z , as function of time, t , with this pulse sequence, for spins remaining in slice for both pulses. C, Effect of varying TD (for fixed velocity) on signal produced by excitation pulse for replacement of "saturated" spins by fully magnetized spins. Solid line shows result for $T_1 = L/v$; broken line shows limit for very long T_1 . D, Effect of increasing velocity (for fixed TD) on signal strength.

the increase is not linear except in the limit of long T_1 . For increasing velocities and a fixed delay time, the signal increases linearly from the signal due to partially saturated stationary spins to a maximum when all the partially saturated spins have been washed out of the slice. Also, note that if the initial saturating pulse were nonselective so that spins outside the slice were equally affected, there would have been no flow effects due to washout, as the spins being washed in by flow would have had an equal degree of saturation.

In multiple-slice excitation, the spins being washed into a slice being imaged may have been previously excited by a selective imaging sequence at another slice location upstream. The degree of saturation of the spins will depend on the history of their prior excitations and on their relaxation time. For a stack of slices being imaged simultaneously, the flow effects on the upstream end of the stack will be the same as for a simple slice, but the slices further downstream will be further affected by the prior excitation of blood being washed in from slices imaged upstream [26].

For SE signal detection, there are additional factors to consider along with washout of saturated spins. The refocusing pulse that produces the spin echo may be selective or nonselective. For a selective refocusing pulse (analogous to a selective excitation pulse) at a time $TE/2$, the signal will be diminished due to washout of excited spins from the refocusing region by a factor of $1 - TEv/(2L)$, as given by equation 1. Thus, the net effect of washout on signal strength for spin echoes may be an increase or a decrease, depending on whether it is the removal of partially saturated spins between excitations or the loss of excited spins before refocusing that dominates (fig. 4).

For a nonselective refocusing pulse, there will be no effects due to loss of excited spins from the refocusing region. However, the 180° nonselective pulse that acts as a refocusing pulse in the slice will act as an inverting pulse upstream,

outside the slice. For a single spin echo, the signal will now only decrease with flow as partially saturated spins in the slice are replaced by even more saturated spins from outside the slice (fig. 5). For SE time, TE , short compared to the pulse sequence repetition time, TR , the steady state ratio of the signal from the spins being washed in from upstream to the signal from any spins remaining in the slice from the previous excitation is given by a factor of about $1/(1 + \exp[-TR/T_1])$ [29] (neglecting the finite extent of the radiofrequency [RF] coil and magnet) and the signal will decrease due to flow as spins within the slice are replaced by more saturated spins from outside the slice. For a finite-length RF coil, there will be an increase in signal if flow is rapid enough to replace spins in the slice with spins from outside the coil (but inside the magnet) during the sequence repetition time. For a pair of spin echoes, the second 180° pulse will return the longitudinal magnetization to close to its initial state, with minimal net effect by the time of the next exciting pulse, for TE s that are short compared to the relaxation time T_1 (fig. 6). Now the saturated spin washout effects of flow will be similar to those shown in figure 3D.

The motion of the excited spins between the time of excitation and the time of SE production may also affect the position of their image, depending on the orientation of the vessel relative to the slice. For flow perpendicular to the slice, the projection of the location of the packet of excited spins onto the slice will be the same at the time of echo production as at the time of excitation, and no displacement effects will be seen in the image. However, for vessels passing obliquely through the plane of the slice, the component of the velocity parallel to the plane of the slice will displace the projection of the location of the excited spins relative to their location at the time of excitation. For a vessel at an angle, A , relative to the plane of the slice, the component of the velocity, v , along the plane of the slice is $v \cdot \cos(A)$ and the displacement of the projection of the spins onto the plane of the slice at the time

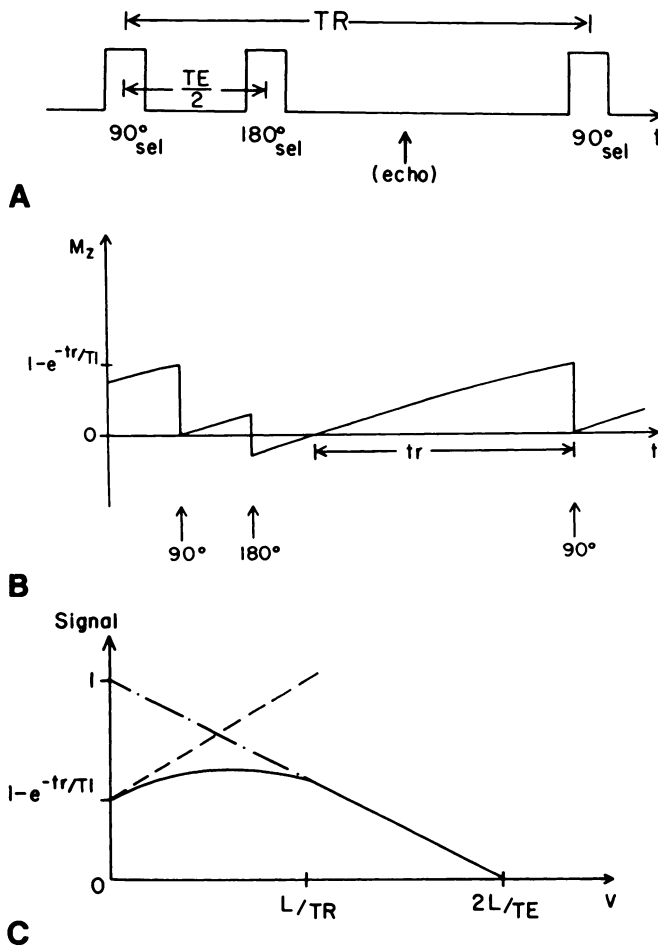


Fig. 4.—Effect of combined washout of saturated and excited spins in imaging with selective spin-echo signal detection. A, Schematic RF pulse sequence: selective 90° excitation pulse followed by selective 180° refocusing pulse with echo formation at time TE; sequence repeats at time interval of TR. B, Effects of this pulse sequence on longitudinal magnetization, M_z , of spins remaining in slice throughout pulse sequence. t_r = time between zero crossing after 180° pulse and the next 90° pulse. C, Effect of increasing velocity (plug flow) on signal strength for replacement of spins in slice by fully magnetized spins. Net signal observed (solid line) is result of combination of effects of replacement of partially saturated spins (broken line) and loss of excited spins from refocusing region (dot-dash line).

of SE production, TE, will be given by $v \cdot \cos(A) \cdot TE$. The visual effect in the image will be a displacement of the image of the signal from the blood relative to the image of the lumen of vessel (fig. 7).

Motion of excited spins through magnetic field gradients, such as are produced for selective irradiation pulses or for position encoding for imaging, results in a phase shift of the spins and signals detected from them. For a magnetic field shift $\Delta B = Gx$ due to a gradient, G, and a constant motion along the direction of the gradient $dx/dt = v$, the phase shift, ϕ , will accumulate at a rate given by $d\phi/dt = \gamma \Delta B = \gamma G(x_0 + vt)$. The net phase shift will thus be given by $\int \gamma G(x_0 + vt) dt$.

The effect of magnetic field inhomogeneities can be approximated in this way by the effect of the equivalent local

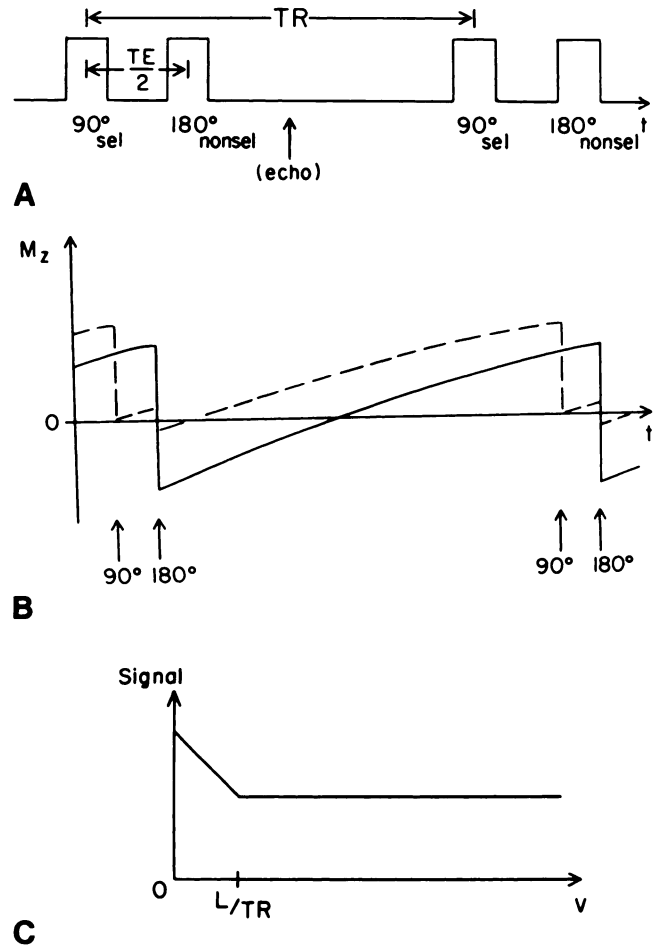


Fig. 5.—Effect of washout with nonselective spin-echo signal detection. A, Schematic RF pulse sequence, as in fig. 4, but with nonselective 180° pulse used to produce echoes. B, Effect of this pulse sequence on longitudinal magnetization for spins remaining in slice (broken line) and spins outside slice (solid line). C, Effect of increasing velocity (plug flow) on signal strength now shows result of replacing spins in slice with more saturated spins from outside.

constant magnetic field gradients (fig. 8). In SE production, there will be a velocity-dependent phase shift of the spins and the resulting signal at the time of the echo $\phi = \gamma Gv(TE/2)^2$ [6]. For a range of velocities, the corresponding range of phases will produce interference between signals from spins with different velocities, with a resulting decrease in amplitude of the signal. If a second spin echo is produced, the phase shifts can be compensated so that the amplitude of the second spin echo may be greater than the first.

Imaging magnetic field gradients are usually applied as pulses. If a pulse of gradient magnetic field of duration, T, is followed immediately by one of appropriate magnitude and opposite polarity, as is commonly used for selective excitation and has been proposed for flow measurement [18, 34], the effect will cancel out for stationary spins, but moving spins will be left with a net phase shift of $\int_0^T \gamma vt \cdot G(t) \cdot dt$ (fig. 9). For square gradient pulse shapes, this is simply given by

γvGT^2 . A second, otherwise identical bipolar gradient pulse with reversed polarity will return the phase shift to zero for constant velocity. Two gradient pulses of equal duration and the same amplitude, one before and one after a 180° refocusing pulse, will have a velocity-dependent effect on the phase of the resulting spin echo similar to that of the bipolar gradient pulse.

A particular example of pulsed-imaging magnetic field gradients that is of interest is the use of selective 180° refocusing pulses. As demonstrated in figure 10, the effect of the selection gradient is to introduce a velocity-dependent phase shift into the first echo (and subsequent odd-numbered echoes)

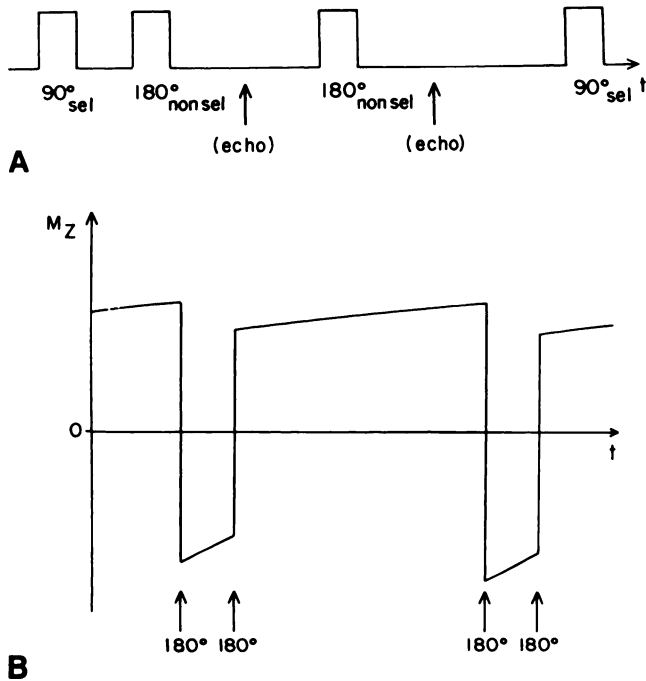


Fig. 6.—Effect of production of pair of nonselective spin echoes on longitudinal magnetization outside slice. A, Schematic RF pulse sequence, as in fig. 5, with second nonselective 180° refocusing pulse. B, Effect of second 180° pulse is to drive longitudinal magnetization back toward its equilibrium value (for sufficiently short TE).

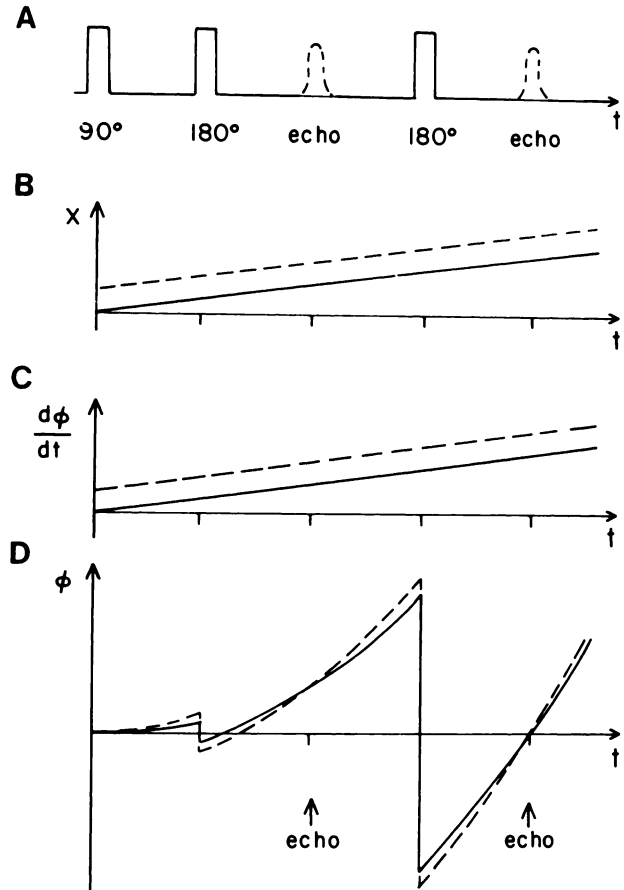


Fig. 7.—Spin-echo formation with flow, v , oblique to plane of slice. A, Initial excitation, 90° pulse. B, Plug of excited spins has partially left slice at time of 180° refocusing pulse. C, At time of spin-echo formation, those excited spins that experienced refocusing pulse have been carried farther out of slice. Projection onto plane of slice of their position (broken lines) will not be in complete registration with position of vessel in slice.

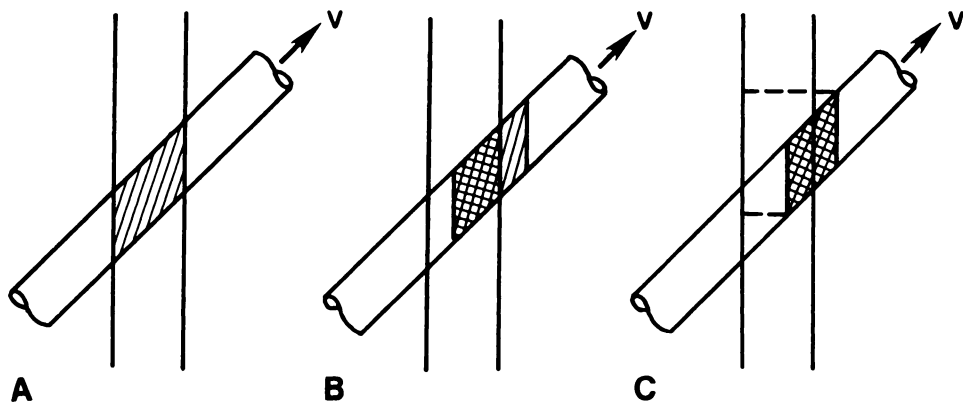


Fig. 8.—Effect of constant velocity motion along constant magnetic field gradient on phase of excited spins. A, Schematic RF pulse sequence with formation of pair of spin echoes (broken lines). B, Position of spins along direction of gradient, x , as function of time, t , for two different initial positions (broken and solid lines). C, Corresponding rate of change of phase, $d\phi/dt$, due to changing local value of magnetic field. D, Net phase accumulated by moving spins. Effect of 180° pulses is to reverse value of phase. Note that at time of echo formation, phase is independent of initial position, but is nonzero (proportional to velocity) for first echo; phase is zero for second echo independent of velocity.

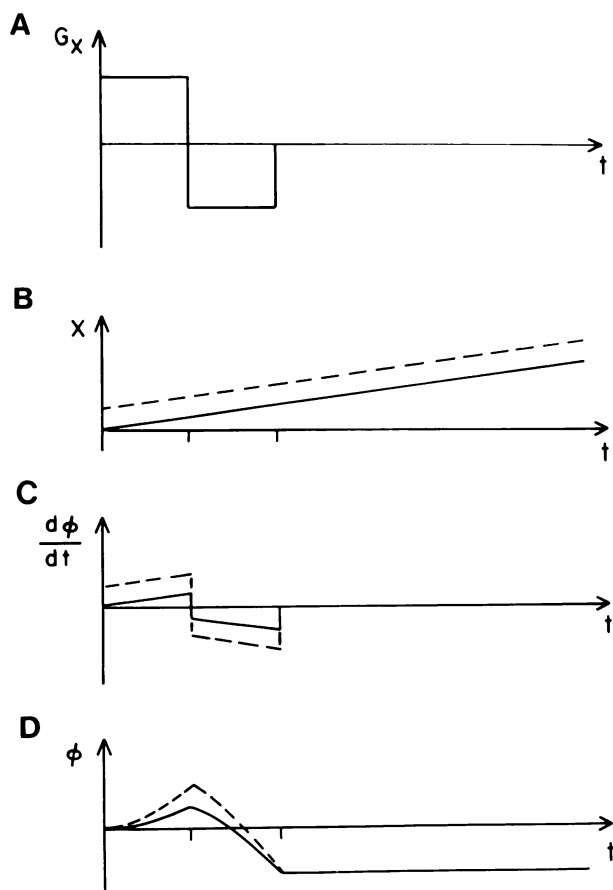


Fig. 9.—Effect of constant velocity motion along bipolar pulsed magnetic field gradient on phase of excited spins. **A**, Schematic gradient pulse sequence. **B**, Position of spins with two different initial positions, as in fig. 8B. **C**, Corresponding rate of change, as in fig. 8C. Note reversal of sign of rate of change corresponding to reversal of gradient. **D**, Net phase accumulated by moving spins. Note that although phase can be adjusted to be independent of initial position ("gradient reversal echo"), it is nonzero (proportional to velocity).

that is cancelled out in the second echo (and subsequent even-numbered echoes).

The distribution of phase shifts, $j(\phi)$, resulting from a particular distribution of velocities, $f(v)$, can be calculated from the formulas above. The resulting reduction of amplitude will be determined by the vector sum of all these phases. For a small range of phases the effect is small, but for a larger range of phase shifts the reduction of amplitude can be significant. Note that in MRI, it is only the range of phases corresponding to the range of velocities in a given pixel that need be considered. Thus, this effect of decreased signal due to phase cancellation may be more prominent away from the center of the image of a large blood vessel; in the center, the velocity gradient is small even though the velocity is maximum.

The effect of pulsatile flow without synchronization of imaging-data acquisition will be to create variable signal strength in different projections, so that the net reconstructed signal within the vessel will only be roughly an average of the different signals. The inconsistency of signal amplitude and

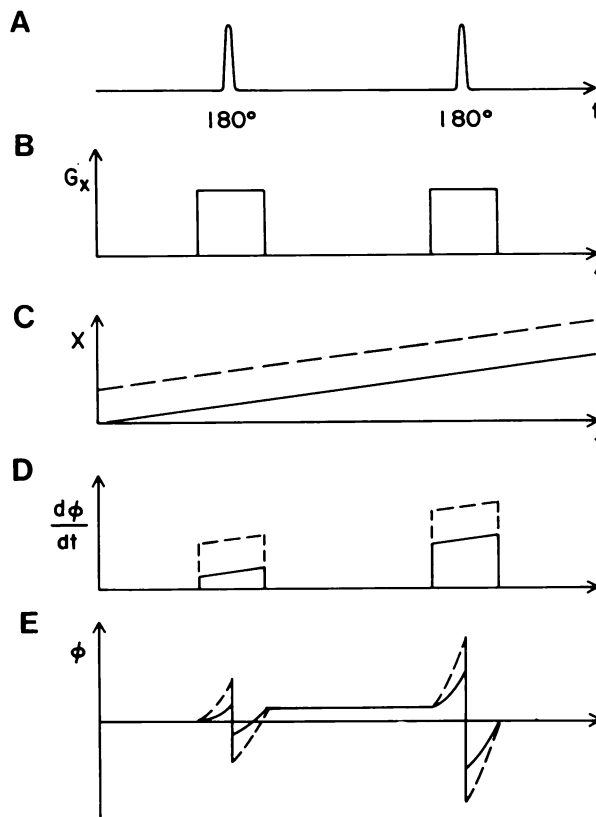


Fig. 10.—Effect of constant velocity motion with selective refocusing pulses on phase of excited spins. **A**, Schematic RF pulse sequence. **B**, Corresponding magnetic field gradient pulse sequence. **C**, Position of spins with two different initial positions, as in fig. 8B. **D**, Corresponding rate of change of phase, as in fig. 8C. **E**, Net phase accumulated by moving spins. Note that phase is proportional to velocity after first refocusing pulse but zero after second pulse.

phase from within the lumina of blood vessels can result in the appearance of signal outside the vessel lumen in the image similar to the effects of respiratory or other patient motion. These effects can be studied by numerical simulations and empirical trials.

Materials and Methods

A phantom study of MR signal intensity as a function of flow velocity was performed in order to illustrate the different flow effects of selective and nonselective refocusing pulses. Tap water with a T1 of 2.8 sec was continuously pumped through Tygon tubing passing through the imaging region of a 0.5-T MRI system. The tubing was coiled loosely in the magnet, upstream from the imaging region to ensure full magnetization of inflowing fluid. Flow rates were measured by timed collections in a calibrated tube; mean velocity was calculated as the ratio of volume flow to the cross-sectional area of the tubing. Rather than taking complete images, the MR signal amplitude was monitored from the peaks of projections of the tubing, obtained by collecting (averaged) signals without a phase-encoding magnetic field gradient. The excitation sequence consisted of a selective (1 cm) 90° excitation pulse followed by either a selective (1 cm) or nonselective 180° refocusing pulse to produce a single spin echo at 17 msec (TE); the TR for this cycle was 300 msec.

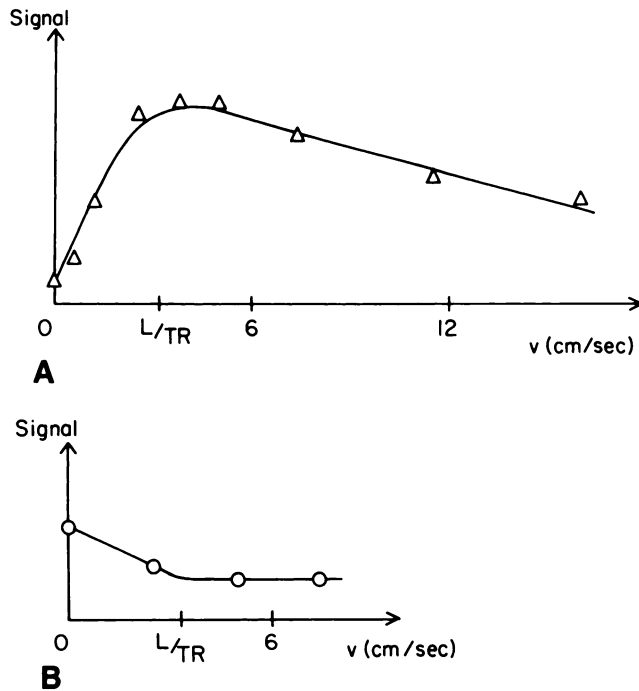


Fig. 11.—Representative results of phantom studies of effects of mean flow velocity, v , on MR signal strength. Slice thickness, L , is 1 cm; pulse sequence repetition time, TR , is 300 msec; echo time, TE , is 17 msec; fluid T_1 is 2.8 sec. Arbitrary signal intensity scale. A, Selective excitation pulse and selective refocusing pulse. B, Selective excitation pulse and nonselective refocusing pulse.

Results

Representative results of the phantom study of dependence of MR signal strength on flow velocity are shown in figure 11. As has been previously reported by others, with a selective refocusing pulse there is an initial increase in signal strength with increasing velocity (the so-called "paradoxical enhancement"), followed by a steady decrease in signal strength with further increase in velocity beyond a rate sufficient to wash out the slice between excitation pulses. This corresponds to the expected effects shown in figure 4C. In contrast, with a nonselective refocusing pulse there is an initial decrease, not increase, in signal strength with increasing velocity, followed by a relatively constant signal intensity for increases in velocity beyond a rate sufficient to wash out the slice between excitation pulses. This corresponds to the expected effects shown in figure 5C. (For flows sufficiently rapid to wash out the region of the RF coil, the signal strength actually increased.)

Discussion

We have seen how the principal blood flow effects in MRI, increased or decreased signal strength and possible displacement of the image of the blood, can be explained in terms of three basic processes: (1) washout of saturated spins from the slice being imaged with replacement by (possibly satu-

rated) spins from upstream, (2) washout of excited spins from the slice being imaged with consequent loss of signal due to incomplete refocusing of spin echoes, and possible displacement of the image, and (3) motion along magnetic field gradients (either part of the imaging process or due to magnetic field inhomogeneity) resulting in phase shifts proportional to the velocity and a consequent decrease in signal for a range of velocities within a picture element. The particular choice of imaging technique used, for example, whether the signal is detected as FID or spin echo, whether refocusing pulses are selective or nonselective, or whether single or multiple planes are imaged simultaneously, will determine the net result in the image of these different flow effects.

The next consideration is how to incorporate these flow effects into imaging techniques designed to produce a quantitative measurement of blood flow (strictly speaking, velocity). The basic idea is that of "tagging" the spins in a selective region, by producing saturation or excitation (with a particular phase), and then looking for flow displacement of the tagged spins at a later time shorter than or on the order of the T_1 or T_2 relaxation time of blood, respectively.

A relatively straightforward way to study flow with imaging would be to measure the washout of saturated spins. Residual saturation remaining in a slice from a preceding selective saturating pulse will reduce the signal produced by a subsequent exciting (imaging) pulse. Increasing the delay time between the saturation (tagging) and exciting (detection) pulses will produce an increasing image intensity in the lumen of the vessel, other factors being kept the same, until all the saturated spins have been swept out of the imaging region in the time between the pulses. Further increases in the delay time should have no further effects on the blood intensity. In order to separate the effects of washout from the effects of recovery of longitudinal magnetization due to the T_1 relaxation time, a comparison image would be made with a nonselective saturating pulse but otherwise identical pulse timing. A variation of this technique would be to displace the selective saturation tagging pulse upstream from the detecting pulse and vary either the time delay between the pulses or their physical separation in order to define the velocity of the blood by detecting the decrease in signal due to arrival of the tagged spins in the imaging plane. A disadvantage of this kind of flow imaging is that it requires a series of images to define the washout curve in order to define the washout time. As with other flow imaging techniques, cardiac synchronization will be necessary to define the full cycle of pulsatile flow. An additional limitation is that only the component of flow perpendicular to the slice will be measured. Thus, it could be very time-consuming to measure blood flow in this way.

The washout of excited spins can be measured very analogously to the washout of saturated spins. In this case, tagging is produced by a selective excitation pulse, and detection is produced by a selective refocusing pulse. Increasing the delay between the exciting and refocusing pulses will result in decreasing signal strength due to loss of excited spins from the imaging region, as described earlier, until all the excited spins have been swept out of the imaging region between pulses and no further signal is detected. In order to

separate the effects of washout from the effects of loss of transverse magnetization due to the T2 relaxation time, a comparison image can be made with nonselective refocusing pulses. A variation on this technique would be to displace the selective refocusing pulses proportionally downstream from the exciting pulse and either vary the timing of the pulses or their physical separation to define the velocity of the blood. As with saturation-washout flow imaging, the need to define the washout curve as well as the other limitations could again result in a time-consuming measurement technique.

A different way to measure the washout of excited spins would be to directly detect their motion by imaging with a frequency-encoding ("readout") gradient along the direction of the motion. For example, using a readout gradient at right angles to the plane of selective excitation will produce an image where spins that have moved due to flow between the time of excitation and signal detection will have a corresponding displacement relative to stationary spins that remain in the slice.

A final class of flow imaging techniques would measure the phase shifts introduced by motion along magnetic field gradients. The use of phase-sensitive image reconstruction will produce varying (baseline) phase shifts due to magnetic field inhomogeneities and imaging gradients. The difference between this baseline phase shift and the phase shift observed with an additional bipolar or paired gradient pulse, balanced as to produce no phase shift for stationary spins, will be due to motion along the flow-encoding gradient and proportional to the velocity. If the gradient is chosen so as to keep the phase shift less than 180° for the highest velocity, the velocity component along the direction of the gradient can be determined directly from the phase shift difference; otherwise a set of images with different gradient strengths will be necessary to sort out the velocities from the phase shift angles. To find the full velocity vector in space, this process can be repeated with gradients applied in the other two orthogonal directions.

With any of the techniques above, what is actually measured is velocity. In order to find total flow in a vessel, the local velocity must be integrated over the cross section of the vessel.

Turbulence, such as downstream from a stenosis, may result in unsteady flow. This will produce variation in intensity from one excitation to another than cannot be corrected with cardiac synchronization. The possibility of recirculating-type vortical flow produced by a stenotic lesion could also increase the time spent in the slice relative to the instantaneous velocity, with a resulting apparent decrease in the measured velocity as determined by washout effects. The phase of an excited spin that has moved out of the plane and back in (due to such vortical flow) may be different from that of adjacent stationary spins.

The washout techniques described above will not be easily extended to the measurement of tissue perfusion, which will not generally produce any net directed velocity. Also, the washout time for tissue is long compared to the relaxation times of blood, so that the effects will be small, in any case, unless very thin sections are tagged. The phase shifts due to motion along gradients will similarly not be seen as a change

in net phase, because of the relatively random direction of tissue flows, but rather will produce a decrease in net signal intensity, similar to the effects of diffusion. Thus, a technique to measure tissue perfusion is most likely to be similar to one to measure the diffusion constant, and it may be difficult to separate the two effects.

ACKNOWLEDGMENTS

I thank John Leigh, Felix Wehrli, James MacFall, and Matthew O'Donnell for helpful discussion; James MacFall and Robert Herfkens helped obtain the experimental data presented.

REFERENCES

1. Caro CG, Pedley TJ, Schroter RC, Seed WA. *The mechanics of the circulation*. New York: Oxford University Press, 1978
2. Folkow B, Neil E. *Circulation*. New York: Oxford University Press, 1971
3. Lassen NA, Perl W. *Tracer kinetic methods in medical physiology*. New York: Raven, 1979
4. Suryan G. Nuclear resonance in flowing liquids. *Proc Indian Acad Sci [A]* 1951;33:107-111
5. Hahn EL. Spin echoes. *Phys Rev* 1958;80:580-594
6. Carr HY, Purcell EM. Effects of diffusion on free precession in nuclear magnetic resonance experiments. *Phys Rev* 1954;94:630-638
7. Singer JR. Blood flow rates by nuclear magnetic resonance measurements. *Science* 1959;130:1652-1653
8. Singer JR. Flow rates using nuclear or electron paramagnetic resonance techniques with applications to biological and chemical processes. *J Appl Phys* 1960;31:125-127
9. Morse OC, Singer JR. Blood velocity measurements in intact subjects. *Science* 1970;170:440-441
10. Grover T, Singer JR. NMR spin-echo flow measurements. *J Appl Phys* 1971;42:938-940
11. Singer JR, Grover T. Recent measurements of flow using nuclear magnetic resonance techniques. In: Clayton CG, ed. *Modern developments in flow measurement*. London: Peter Peregrinus, 1972:38-47
12. Battocletti JH, Halbach RE, Salles-Cunha SX, Sances A. The NMR blood flowmeter—theory and history. *Med Phys* 1981;8:435-443
13. Halbach RE, Battocletti JH, Salles-Cunha SX, Sances A. The NMR blood flowmeter—design. *Med Phys* 1981;8:444-451
14. Salles-Cunha SX, Halbach RE, Battocletti JH, Sances A. The NMR blood flowmeter—applications. *Med Phys* 1981;8:452-458
15. Jones DW, Child TF. NMR in flowing systems. In: Waugh JJ, ed. *Advances in magnetic resonance*. New York: Academic, 1976:123-148
16. Singer JR. NMR diffusion and flow measurements and an introduction to spin phase graphing. *J Phys E* 1978;11:281-291
17. Hahn EL. Detection of sea-water motion by nuclear precession. *J Geophys Res* 1960;65:776-777
18. Stejskal EO. Use of echoes in a pulsed magnetic-field gradient to study anisotropic, restricted diffusion and flow. *J Chem Phys* 1965;43:3597-3603
19. Arnold DW, Burkhart LE. Spin-echo NMR response from a flowing sample. *J Appl Phys* 1965;36:870-871
20. Packer KJ. The study of slow coherent molecular motion by pulsed nuclear magnetic resonance. *Molecular Phys*

- 1969;17:355-368
21. Hayward RJ, Packer KJ, Tomlinson DJ. Pulsed field-gradient spin echo. N.M.R. studies of flow in fluids. *Molecular Phys* **1972**;23:1083-1102
 22. Garroway AN. Velocity measurements in flowing fluids by NMR. *J Phys D* **1974**;7:L159-L163
 23. Hinshaw WS, Bottomley PA, Holland GN. Radiographic thin-section image of the human wrist by nuclear magnetic resonance. *Nature* (London) **1977**;270:722-723
 24. Young IR, Burl M, Clarke GJ, et al. Magnetic resonance properties of hydrogen: imaging the posterior fossa. *AJR* **1981**;137:895-901
 25. Crooks L, Sheldon P, Kaufman L, Rowan W, Miller T. Quantification of obstructions in vessels by nuclear magnetic resonance (NMR). *IEEE Trans Nucl Sci* **1982**;NS-29:1181-1185
 26. Kaufman L, Crooks LE, Sheldon PE, Rowan W, Miller T. Evaluation of NMR imaging for detection and quantification of obstructions in vessels. *Invest Radiol* **1982**;17:554-560
 27. Crooks LE, Hoenninger JC, Arakawa M. Pulse sequences for NMR imaging using multidimensional reconstruction techniques. In: Partain CL, ed. *Nuclear magnetic resonance and correlative imaging modalities*. New York: Society of Nuclear Medicine, **1984**:69-74
 28. Grant JP, Back C. NMR rheotomography: feasibility and clinical potential. *Med Phys* **1982**;9:188-193
 29. Wehrli FW, MacFall JR, Axel L, Shutts D, Glover GH, Herfkens RJ. Approaches to in-plane and out-of-plane flow imaging. *Non-invasive Med Imaging* **1984**;1:127-136
 30. Crooks LE, Mills CE, Davis PL, et al. Visualization of cerebral and vascular abnormalities by NMR imaging: the effects of imaging parameters on contrast. *Radiology* **1982**;144:843-852
 31. Herfkens RJ, Higgins CB, Hricak H, et al. Nuclear magnetic resonance imaging of the cardiovascular system: normal and pathologic findings. *Radiology* **1983**;147:749-759
 32. Singer JR, Crooks LE. Nuclear magnetic resonance blood flow measurements in the human brain. *Science* **1983**;221:654-656
 33. Axel L. Approaches to nuclear magnetic resonance (NMR) imaging of blood flow. *Proc SPIE* **1982**;347:336-341
 34. Moran PR. A flow velocity zeugmatographic interlace for NMR imaging in humans. *Magnetic Resonance Imaging* **1982**;1:197-203
 35. Van Dijk P. Direct cardiac NMR imaging of heart wall and blood flow velocity. *J Comput Assist Tomogr* **1984**;8:429-436
 36. Bryant DJ, Payne JA, Firmin DN, Longmore DB. Measurement of flow with NMR imaging using a gradient pulse and phase difference technique. *J Comput Assist Tomogr* **1984**;8:588-593
 37. O'Donnell M. NMR blood flow imaging using multi-echo, phase contrast sequences. *Med Phys* **1985**;12 (in press)
 38. Feinberg DA, Crooks L, Hoenninger J, Arakawa M, Watts J. Visualization of pulsatile blood velocity in human arteries by magnetic resonance imaging. *Radiology* (in press)
 39. George CR, Jacobs G, MacIntyre WJ, et al. Magnetic resonance signal intensity patterns obtained from continuous and pulsatile flow models. *Radiology* **1984**;151:421-428